Combust. Sci. and Tech., 1998, Vol. 139, pp. 207–227
Reprints available directly from the publisher
Photocopying permitted by license only

© 1998 OPA (Overseas Publishers Association) N.V.
Published by license under
the Gordon and Breach Science
Publishers imprint.
Printed in Malaysia.

Development of a Lean Premixed Low-Swirl Burner for Low NO_x Practical Applications

D. T. YEGIAN and R. K. CHENG*

Environmental Energy Technologies Division, Ernest Orlando Lawrence Berkeley National Laboratory, Berkeley, CA 94720

(Received 15 December 1997; In final form 26 August 1998)

Laboratory experiments have been performed to evaluate the performance of a premixed low-swirl burner (LSB) in configurations that simulate commercial heating appliances. Laser diagnostics were used to investigate changes in flame stabilization mechanism, flowfield, and flame stability when the LSB flame was confined within quartz cylinders of various diameters and end constrictions. The LSB adapted well to enclosures without generating flame oscillations and the stabilization mechanism remained unchanged. The feasibility of using the LSB as a low NO_x commercial burner has also been verified in a laboratory test station that simulates the operation of a water heater. It was determined that the LSB can generate NO_x emissions < 10 ppm (at 3% O_2) without significant effect on the thermal efficiency of the conventional system. Our study has demonstrated that the lean premixed LSB has commercial potential for use as a simple economical and versatile burner for many low emission gas appliances.

Keywords: Premixed; swirl; NO_x; practical system

INTRODUCTION

Since its inception (Chan *et al.*, 1992), the low-swirl burner (LSB) has been a useful research burner for fundamental studies of premixed turbulent flames (Chan, 1992; Bedat and Cheng, 1995; Cheng, 1995; O'Young and Bilger, 1996). The LSB can operate under wide ranges of equivalence ratios (ϕ), thermal inputs, and turbulence intensities. The flame produced by a LSB is

*Corresponding author.

lifted and detached from the burner (Fig. 1), and thus allows easy access for laser diagnostics throughout the pre- and post-combustion zone. It is also axisymmetric and propagates normal to the incident reactants. Therefore, the LSB is well suited for investigating empirical coefficients such as flame speed, turbulence transport, and flame generated turbulence.

Bedat and Cheng (1995) used a LSB to conduct a systematic investigation of flame structures in moderate to intense turbulence ($u'/S_l = 2-12$). From Rayleigh scattering, they found flamelet characteristics well within the distributed reaction zone regime. In a subsequent paper, Cheng (1995) demonstrated that lean turbulent premixed flames ($\phi \leq 0.7$) do not exhibit the so-called 'counter-gradient' behavior. Other studies using a LSB include the work by O'Young and Bilger (O'Young and Bilger, 1996) on scalar dissipation, and the report by Bedat *et al.* (Bedat and Cheng, 1996) on turbulent flame wrinkle structures. The LSB also holds significance for numerical modeling and combustion theory. As the low-swirl stabilization mechanism is different from the conventional high-swirl mechanisms (Beer, 1996) modeling of the LSB flowfield may require full treatment of the three dimensional momentum equation with mean radial and axial pressure gradients.

Due to its capability to stabilize ultra-lean premixed flames, the LSB has generated interest from the gas appliance industry for use as an economical

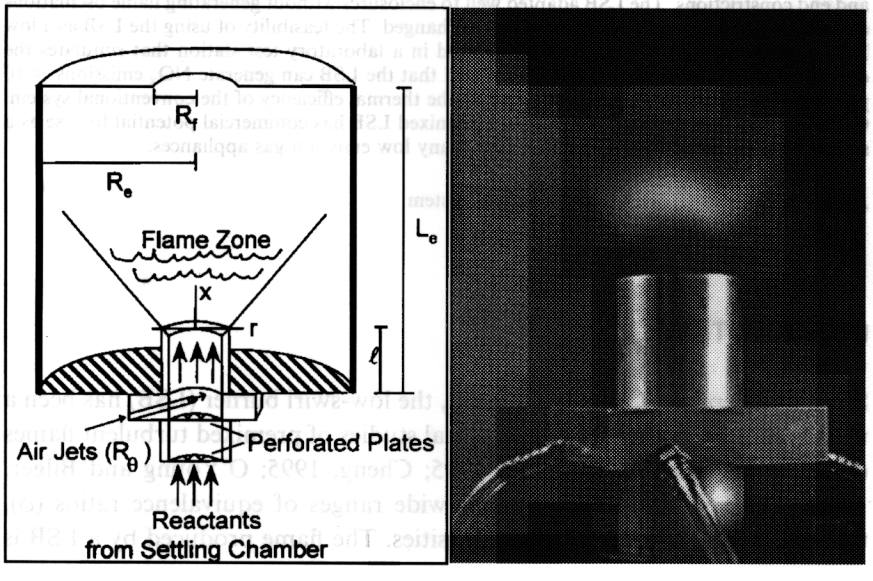

FIGURE 1 Schematic of the Low Swirl Burner and its operation.

low-NO_x burner. Due primarily to the low flame temperatures generated by lean premixed combustion, NO_x emissions can be as low as a few ppm (Bowman, 1992), thus eliminating the need for emission reduction methods such as catalysts, fuel–air staging, or flue gas recirculation. In the gas turbine industry, substantial research efforts have already been undertaken to develop lean premixed combustors. For commercial and residential applications, premixed pulsed combustors (Keller *et al.*, 1994) and premixed ceramic matrix burners (Williams *et al.*, 1992) are available and have been demonstrated to achieve low NO_x. Both technologies, however, have limitations that restrict them from broad use. The non-linear, acoustic feedback coupling process in pulsed combustors makes scaling to different thermal inputs and geometries quite challenging. The ceramic matrix burner is costly, fragile, and heavy, and so it may not be economically feasible for many consumer and commercial heating products.

The practical advantage of the LSB is its design simplicity and wide operating range. A 52.8 mm diameter burner operates up to at least 55 kW (Bedat and Cheng, 1995), and has a turn-down ratio of at least 10 to 1. The purpose of this study is to investigate the feasibility of using a LSB in small boilers/furnaces by conducting laboratory experiments that simulate the operating conditions and environment of practical systems. Typically, the burner (or burners) in these systems fire directly into a 'sealed' furnace chamber with a constricted exhaust. The heat exchanger is usually fitted within this chamber. The furnace chambers can be quite large to accept multi-burners or sufficiently small to confine and influence the flame. One important developmental issue for boilers and furnaces is how a burner behaves and performs in different chamber geometries.

For strong swirl burners, there are several publications on how the confinement of the furnace affects flame oscillations, heat transfer, and emissions (Heitor *et al.*, 1984; Schefer *et al.*, 1996). The open duct experiments of Heitor (1984), Halthore and Gouldin (1986), and Sivasegaram and Whitelaw (1987) show that the flame stabilization regime is sensitive to the swirl intensity, enclosure size and the placement of the bluff-body. With a constricted exhaust, several studies (Sivasegaram and Whitelaw, 1991; Richards, *et al.*, 1997) show that the combustion chamber becomes a Helmholtz resonator and can generate noise and other destabilizing, or even destructive, effects.

Since the LSB flame is detached and freely propagating, it is critical to understand how it responds to confinement and exhaust constriction. To study these effects in the laboratory, quartz cylinders of various diameters and lengths were used to confine the flame and an exhaust plate with a small

center opening ($R_f = R$) was used as an exhaust constriction. Using a quartz cylinder allowed for the application of laser diagnostics to measure flame properties and flowfield characteristics. Encouraged by the performance in these enclosures, the LSB was further evaluated in a water heater simulator that consisted of a LSB fitted within a commercial spa heater of 15 kW (50,000 Btu/hr.). Thermal efficiency and emission levels (NO_x, CO and O_2) were used as performance indicators for the experiments which included different thermal inputs and equivalence ratios. The test results are very encouraging and confirm the potential of the LSB as an economical low-emission burner for combustion applications.

BACKGROUND

The use of high swirl for flame stabilization is common in gas turbines, dump combustors and industrial furnaces (Syred and Beer, 1974). It is most effective for very high speed flows by offering a means to control flame intensity, size and shape. Generally, swirling motion is created by tangential air injection or by guide-vanes fitted within an annular region that surrounds a fuel rod. In a conventional swirl burner, the significant role of swirl is to create a torroidal recirculation zone (TRZ). To prompt the formation of a TRZ, a centered bluff body is often used in conjunction with a swirling annular flow. For non-premixed combustion, the TRZ promotes mixing of fuel and air for more complete combustion, and stabilizes the flame by recirculating the hot combustion products. For premixed combustion, the TRZ generates a zone of hot combustion products that enables the flame to anchor at the upstream or the downstream stagnation points. The mechanisms of TRZ flame stabilization have been the subject of numerous review papers (Syred and Beer, 1974; Lilley, 1977).

In contrast, there are only a few early studies on using non-recirculating swirl flows for flame stabilization (Chigier and Chervinsky, 1966). Activities in this area waned because a TRZ was deemed to be more reliable for flame stabilization. The difference between the early low-swirl studies and our current work is the experimental configuration and jet Reynolds number. Chigier *et al.*, 1966) studied the effects of a large amount of weakly swirling co-flow air that surrounded a small rich premixed jet ($Re \approx 200000$). As this jet was supplied by a fully developed, turbulent pipe flow, weak swirl only influenced the jet's periphery and not the high-speed core. This configuration generated a partially burned, lifted flame that anchored at the jet's

perimeter. A large portion of reactants escaped though the center without burning.

The LSB uses a large diameter jet at a much lower Reynolds number, $Re \approx 10000$, with an initial uniform, plug flow profile. The high velocity annular swirl jets create a radial mean pressure gradient that uniformly diverges the plug flow. This configuration enables the flame to propagate upstream against the decelerating divergent flow and stabilize itself at the position where the local flow velocity equals the flame speed. The LSB flames do not easily blow-off as the flow downstream of the flame zone is slower than the flame speed, while flashback occurrences are limited as the flow upstream of the flame front is faster than the flame speed.

In Beer and Chigier (1972), a swirl number for characterizing the swirl intensity is approximated as:

$$S \equiv \int_0^R UWr^2 dr \Big/ R \int_0^R U^2 r dr \tag{1}$$

When tangential injection is used, a geometric swirl number

$$S_g \equiv \frac{R_\theta * R * \pi}{A_\theta} \left(\frac{m_\theta}{m_t} \right)^2 \tag{2}$$

has been defined (Claypole and Syred, 1980) to allow for the calculation of swirl intensity without direct measurements of angular and axial velocities. The term "strong swirl" is applied to those burners with $S_g \geq 0.6$ as the onset of recirculation occurs at this level of swirl intensity. Since the LSB stabilizes a flame without using recirculation as a means of stabilization, S_g is expected to be below 0.6.

APPARATUS AND DIAGNOSTICS

The schematic of the low-swirl burner (LSB) with an enclosure and the optional exhaust constriction is shown in Figure 1. The burner tube has a radius, R of 26.4 mm and is mounted on a converging nozzle attached to a settling chamber. As the premixture enters the burner through the converging nozzle, two perforated screens (hole diameter 3.2 mm) generate turbulence (6–8%) in the flow. Four jets (R_θ = 1.6 mm) inject the swirl air tangentially (inclined 20° from horizontal) to the perimeter of the fuel/air premixture. As the swirl air is distributed only to the flow periphery and does not dilute the core flow, ϕ is reported here without including the swirl air contribution. The length of the exit tube, ℓ, determines the interaction

time of the swirl air with the premixture and therefore affects the stabilization limits. For this study, we used exit tubes with the length, ℓ, ranging from 20 mm to 120 mm and the exit rims tapered to 45° to guide the formation of a divergent flow.

The dimensions of the quartz cylindrical ducts (radii, R_e and lengths, L_e) used to create the combustion chamber are listed in Table I. The exit constriction consisted of a plate with an opening $R_f = 26.4$ mm which was placed on top of the quartz cylinder. This construction area ratio, about 11% of the combustion chamber cross section area, is more severe than that found in most commercial heaters. Two turbine meters were used to monitor the flow rates of air and methane, while the flow rate of swirl air was monitored with the use of a manometer.

Two component laser Doppler velocimetry (LDV) and Mie-scattering-from-oil-droplets (MSOD) were used for measuring velocities and flame crossing spectra. These techniques have been used in previous studies (Bedat and Cheng, 1995; Cheng, 1995). The LDV is a four-beam, two color (514 and 488 nm) system with 5 MHz differential shifting frequency for the axial component and 2 MHz for the transverse component. Unconditional mean (U, V, and W) and rms (u', v', and w') velocities were measured using 0.05 micron Al_2O_3 seed particles. At each position, 1024 co-validated samples were collected using a 10 μsec co-validation criterion.

The MSOD optics are integrated into the LDV system with an additional photomultiplier to monitor Mie scattering from the 488 nm beams. As the oil aerosol burns and evaporates at the flame front, within the turbulent flame brush, the MSOD signal resembles a random telegraph signal. The MSOD signal was sampled at 5 kHz with 2.4 Hz bandwidth. Fast Fourier Transformation (FFT) of the signals produced flame crossing spectra that were used to infer if flame oscillations occurred within the enclosure. Such oscillations can destabilize the flame and generate noise. The signals were also analyzed to determine the mean progress variable, $\bar{c}$.

Figure 2 shows a schematic of the water heater simulator which uses a chamber/heat-exchanger assembly from a Teledyne Laars Telstar Spa

TABLE I Test configurations for the LSB

Designation	*Description*	R_e (*mm*)	R_e/R	L_e (*mm*)	L_e/R	R_f (*mm*)
Case A	Open	n/a	n/a	n/a	n/a	n/a
Case B1	Enclosed	78	3	300	12	n/a
Case B2	Enclosed	78	3	200	8	n/a
Case B1c	Enclosed, constricted	78	3	300	12	26.4
Case B2c	Enclosed, constricted	78	3	200	8	26.4
Case C	Enclosed	47.5	2	260	10	n/a

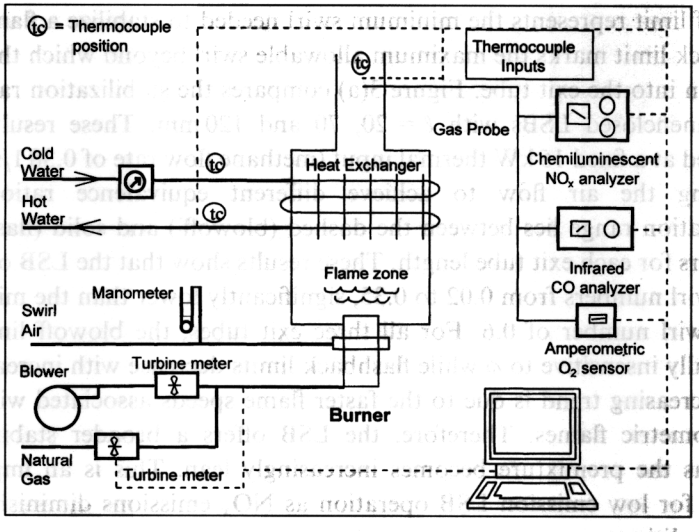

FIGURE 2 Schematic of the laboratory water heater simulator.

Heater rated at 15 kW (50,000 Btu/h). This assembly is 200 × 165 × 230 mm and has a flue radius of 50 mm. The LSB described above is fitted to the sealed bottom of the assembly with the exit tube protruding 30 mm into the chamber. The heat exchanger is of fin-and-tube design and is situated 160 mm above the LSB rim. The flue duct is 500 mm long with a stainless steel sampling port 40 mm below the exit. The exhaust sample passes through a water trap and a desiccant chamber before being split and sent into a chemilumenescent NO-NO_2-NO_x analyzer, and infrared CO analyzer, and an amperometric O_2 process monitor. The thermal efficiency of the system is determined using two calibrated mercury thermometers (+/ − 0.1°C) to measure the input and output water temperatures. Six Type T thermocouples monitored the temperature of the exhaust products and ambient air, as well as water temperatures at different positions along the flow path of the heat exchanger.

RESULTS AND DISCUSSION

Stabilization Range

The stabilization range of the LSB is defined by the blowoff and flashback swirl number, S_g, for different equivalence ratios and thermal inputs. The

blowoff limit represents the minimum swirl needed to stabilize a flame. The flashback limit marks the maximum allowable swirl beyond which the flame is drawn into the exit tube. Figure 3(a) compares the stabilization ranges of three unenclosed LSBs with $\ell = 20$, 70 and 120 mm. These results were obtained at a fixed 15 kW thermal input (methane flow rate of 0.38 1/s) while adjusting the air flow to achieve different equivalence ratios. The stabilization range lies between the dashed (blowoff) and solid (flashback) line pairs for each exit tube length. These results show that the LSB operates with swirl numbers from 0.02 to 0.35, significantly lower than the minimum TRZ swirl number of 0.6. For all three exit tubes, the blowoff limits are essentially insensitive to ϕ while flashback limits decrease with increasing ϕ. The decreasing trend is due to the faster flame speeds associated with near stoichiometric flames. Therefore, the LSB offers a broader stabilization range as the premixture becomes increasingly lean. This is an important feature for low emission LSB operation as NO_x emissions diminish under lean conditions.

The results of Figure 3(a) also show that although the longer exit tubes have higher swirl requirements, they also offer wider stabilization ranges.

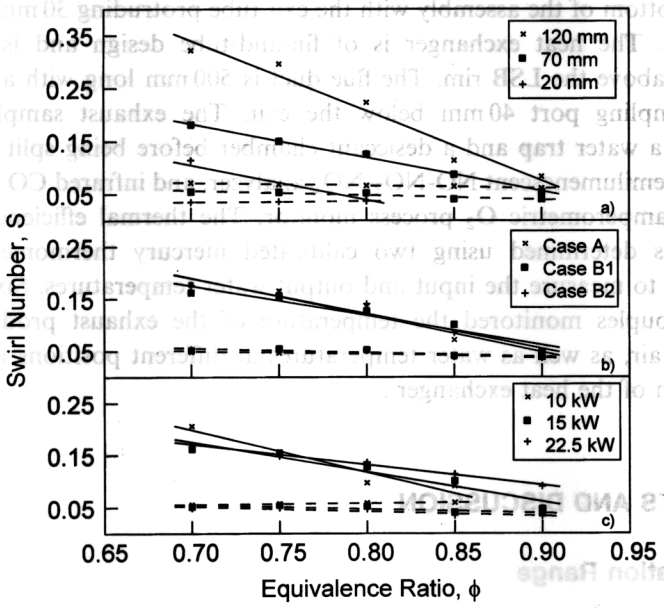

FIGURE 3 Blowoff and flashback limits (·····/——) for (a) various exit tube lengths ℓ; (b) Cases A, B1 and B2; and (c) various thermal inputs.

The LSB with the shortest exit tube, $\ell = 20$ mm can only operate below $\phi < 0.8$ and its limited S_g range seems to be too restrictive for practical use. A longer exit tube prolongs the residence time for the swirl air to interact deeper into the core of the flow. This causes a loss in angular momentum and so an increase in swirl air is needed to generate the necessary divergent flow for flame stabilization. As the $\ell = 70$ mm burner generates a stable flame, operates up to $\phi = 0.9$ at 15 kW and has relatively low swirl requirements, it was used for all other experiments.

Figure 3(b) compares the stabilization ranges of the open and enclosed LSBs at 15 kW with $\ell = 70$ mm. As seen, the large radius enclosures (Cases B1 and B2) have almost no effect on blowoff and flashback limits. The stabilization range of Case C was also investigated but the results are not shown because blowoff limits were ambiguous in this smaller enclosure. While reducing the swirl air to induce blowoff, the flame would become anchored near the enclosure walls such that the flame remained stable within the cylinder but through an entirely different stabilization process. Flashback limits for Case C were not significantly different that those shown in Figure 3(b).

The impact of thermal input on swirl requirement for Case A ($\ell = 70$ mm) is shown in Figure 3(c). A broader stabilization regime becomes accessible at higher thermal inputs as the slopes for the flashback limits decrease with increases in thermal input. With the reference velocity U_∞ only slightly higher than the flame speed at the intersection point of $\phi = 0.85$, 10 kW is the minimum practical thermal input for a LSB with $R = 26.4$ mm. For higher thermal inputs, U_∞ is significantly higher than the flame speed and the operating range extends to $\phi = 0.9$ at 15 kW and to above stoichiometry, where the maximum flame speeds are attained, at 22.5 kW.

Flowfields of Open and Enclosed Flames

Figure 4 shows 2D vector plots obtained in non-reacting and reacting flows of the open LSB (Case A) and two enclosed LSBs (Cases B1 and C). These flows were maintained at $S_g = 0.05$ and $U_\infty = 3.0$ m/s, which corresponds to a thermal input of 18.5 kW when $\phi = 0.80$ for the reacting flow. The non-reacting flowfields are shown on the left, and the corresponding reacting flowfields are shown on the right. The flame zones are delineated at $\bar{c} = 0.1$, 0.5 and 0.9. Although swirl flows are inherently three dimensional, the 2D $U-V$ vector plots are suitable for comparing axisymmetric features of the LSB flowfields such as flow divergence and recirculation (Bedat and Cheng, 1995).

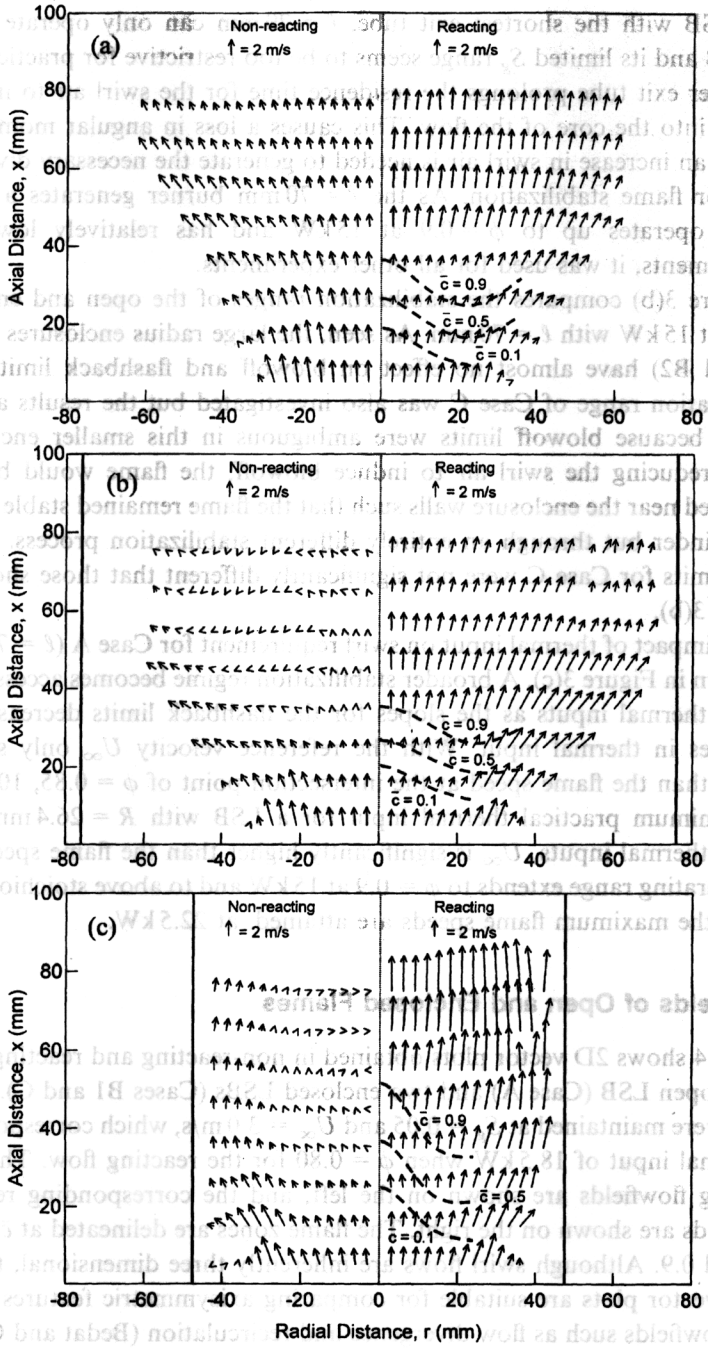

FIGURE 4 2D rector plots obtained in non-reacting and reacting flows at $S_g = 0.05$, $U_\infty = 3.0$ m/s, and $\phi = 0.80$ for (a) Case A; (b) Case B1; and (c) Case B2.

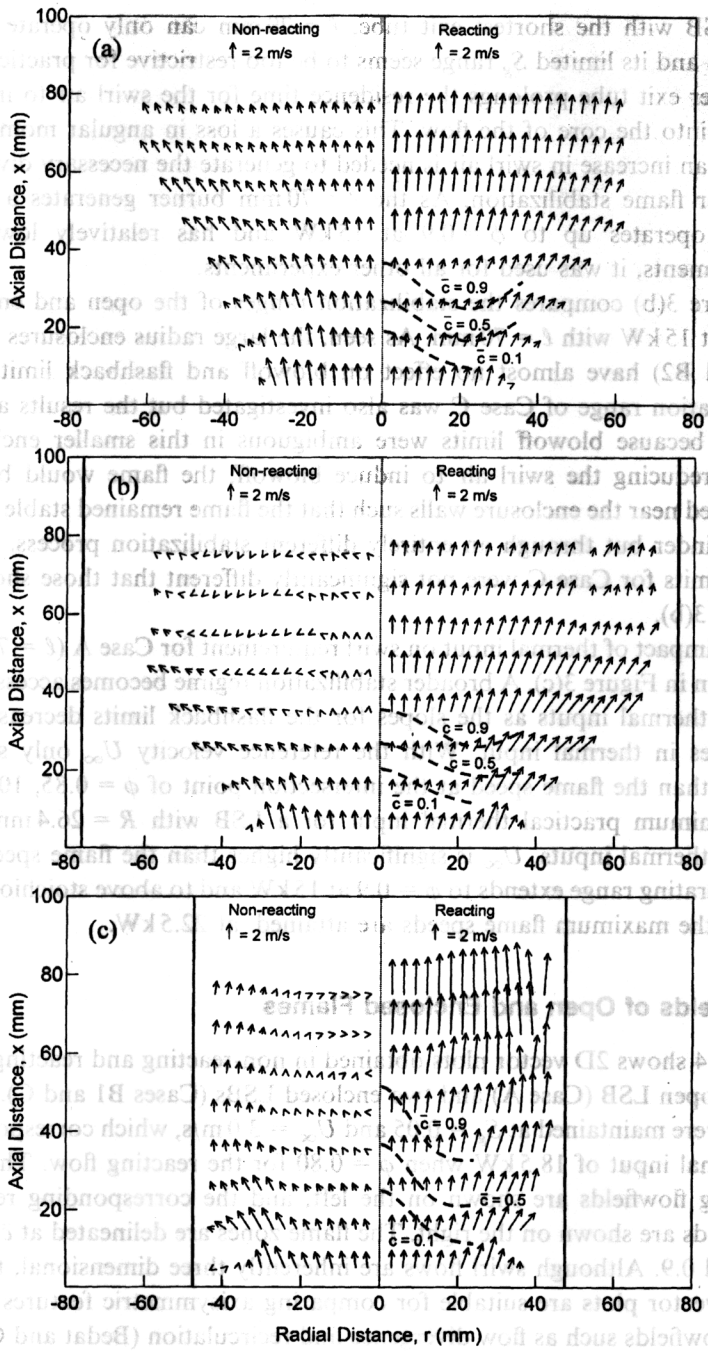

FIGURE 4 2D rector plots obtained in non-reacting and reacting flows at $S_g = 0.05$, $U_\infty = 3.0$ m/s, and $\phi = 0.80$ for (a) Case A; (b) Case B1; and (c) Case B2.

The open LSB (Fig. 4(a)) serves as the reference for Case B1 (Fig. 4(b) and Case C (Fig. 4(c)). In Figure 4(a), the velocity vectors show that the differences between the non-reacting and reacting flowfields of an open LSB occur mostly downstream of the flame where combustion induced flow acceleration takes place. The use of the larger enclosure (Case B1, (Fig. 4(b)) affects both the non-reacting and the reacting flowfields. Compared to the open LSB, the non-reacting axial velocities are reduced substantially for $x > 30$ mm. This reduction can be explained by the process of flow divergence. With a cross-sectional area ratio of $R_e/R = 3$, uniform divergence of a flow with $U_\infty = 3$ m/s would reduce the mean axial velocity to 0.33 m/s. This is the magnitude found near the centerline at $x = 40$ mm. Further downstream at $x > 60$ mm, the non-reacting flowfield is less uniform and there are some areas of flow reversals. These areas of flow reversals are not present in the reacting flowfield, shown on the right, where a uniform flow of products with higher velocities is found. Although the flame zone for Case B1 is located about the same position as for Case A, the $\bar{c}$ contours indicate that the flame brush is slightly flattened. A higher radial mean stretch, displayed by the flow vectors downstream of the flame zone, may be the cause of this phenomenon.

With a tighter enclosure ($R_e/R = 2$), the non-reacting flowfield in Figure 4(c) shows features that resemble the leading edge of a very large and long recirculation zone centered on the cylinder axis. A small outer recirculation zone is also found near the juncture of the cylinder wall and enclosure bottom at $x = 5$ mm and $r > 35$ mm. However, as none of these features are present in the reacting flowfield, recirculation plays no role in the stabilization of this flame. Due to the smaller enclosure diameter, it is to be expected that the flow velocities downstream of the flame zone in Figure 4(c) are higher than those found in Cases A and B1. The $\bar{c}$ contours show that although combustion starts at approximately $x = 20-25$ mm for all three cases ($r = 0$), the Case C flame is significantly thicker with the on-axis, trailing edge of the flame brush 15–20 mm higher than either Case A or B1.

A more detailed comparison of the three reacting cases is provided by the centerline profiles of Figure 5. The mean axial velocity profiles (Fig. 5(a)) are characterized by an initial linear decrease associated with flow divergence in the reactants ($x \leq 15$) followed by combustion generated acceleration in the flame zone ($0 < \bar{c} < 1$). As expected, the velocity profiles for Cases A and B1 are similar. The mean strain rate, a, upstream of the flame zone ($5 \leq x \leq 15$ mm) is 29.8/s and 30.2/s for Case A and B1 respectively. The small difference lends further support to the notion that the minor change in the flame shape as shown in Figure 4(a) and (b) is associated with

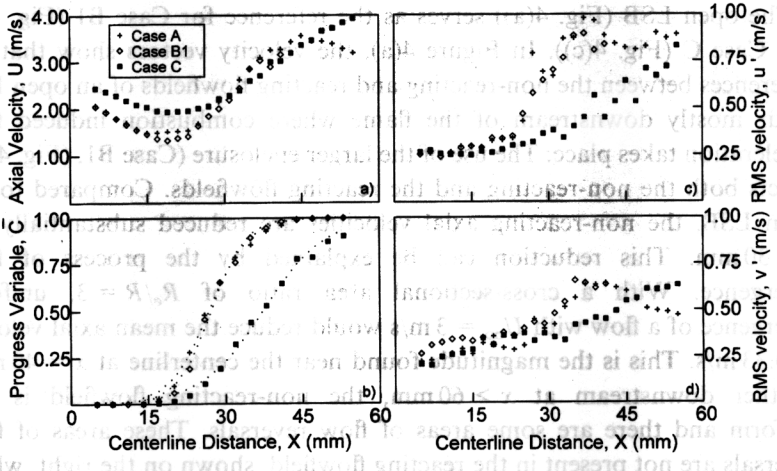

FIGURE 5 Mean velocity (U), progress variable ($\bar{c}$), and rms velocities (u' and v') profiles for Cases A, B1 and B2 with $S_g = 0.05$, $U_\infty = 3.0$ m/s and $\phi = 0.80$.

downstream, rather than upstream, effects. For Case C, the smaller enclosure constrains the flow divergence such that $a = 21.0$/s.

The centerline $\bar{c}$ profiles of Figure 5(b) reveal in greater detail the thickening of the flame brush due to the tighter enclosure (Case C). Determined by the maximum gradient method, the flame brush thickness $\delta = 23.8$ mm for Case C while $\delta = 15.0$ mm and 13.1mm for Case A and Case B1. Even though the leading edges of the flame brushes are within 3 mm of each other, $U_{\min}$ (1.94 m/s) at the leading edge of the Case C flame brush is higher than either Case A or B1 ($U_{\min} = 1.48$ m/s and 1.36 m/s). Figures 5(c) and (d) show the rms velocities u' and v'. Again, the profiles for data from Case A and Case B1 are similar while for Case C the locations of the u' and v' peaks are shifted further downstream due to the thickening of the flame brush for Case C. The magnitudes of the rms velocities in the post flame region are comparable for all three cases.

This velocity data shows that the divergent nature of the LSB adapts well to enclosures of different sizes. A cylinder wider than the open flame brush (*e.g.*, Case B) does not significantly affect the overall flow features. A tighter enclosure (Case C) causes the non-reacting flow to form a large but weak recirculation zone. However, combustion generated flow acceleration easily overcomes and removes these large flow structures, leaving the flame stabilization mechanism unaffected. Although stable operation is achievable for Case C, the smaller enclosure was not chosen for further tests as it seemed to overly confine the flame brush.

Exhaust Constriction Effects

The effects of exhaust constriction are shown by the centerline mean and rms velocity profiles obtained for Cases A, B1, B2, B1c and B2c with $U_\infty = 2.7$ m/s, $S_g = 0.05$ and $\phi = 0.80$ (Fig. 6). As the exit tube extends 50 mm into the enclosure, the enclosure terminates at $x = 250$ mm for Case B1 and B1c, and at $x = 150$ mm for Case B2 and B2c. All the profiles have similar features up to the trailing edge of the turbulent flame brush ($x \approx 50$ mm). The only observable change is that the exhaust constriction pushes the flame zones slightly upstream as seen in both the mean and rms velocity profiles.

Differences in the mean velocity profiles are found downstream of the flame zones. For the unenclosed flame (Case A), the mean velocity in the post flame region remains relatively constant at about 3.0 m/s. This is due to the non-diverging nature of the exhaust plume as shown earlier in Figure 4(a). All the enclosed cases show the products decelerating just downstream of the flame due to the exhaust plume expanding to fill the enclosure. Changes in the mean velocity profiles due to exhaust constriction were only observed for Case B2c ($L_e = 200$ mm), with the products accelerating when $x > 100$ mm. With the constriction further downstream (Case B1c,

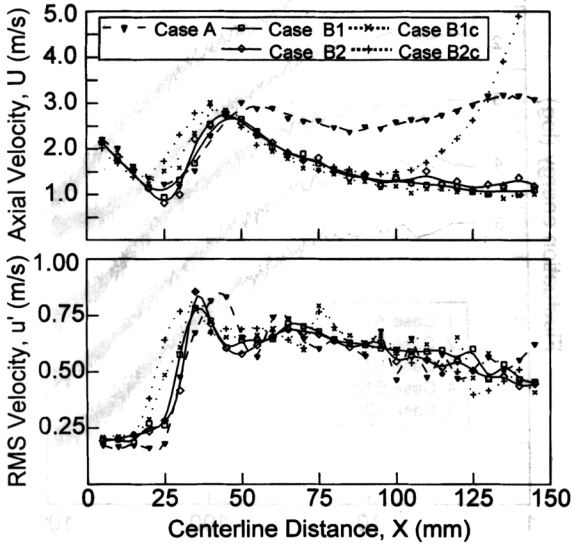

FIGURE 6 Mean (U) and rms (u') centerline velocity profiles for Cases A, B1, B2, B1c and B2c with $S_g = 0.05$, $U_\infty = 2.7$ m/s and $\phi = 0.80$.

$L_e = 300$), no flow acceleration is found. The rms axial velocity profiles of Figure 6 show no significant impact due to enclosure length or exhaust restriction. These results demonstrate that exhaust constriction does not have a significant effect on flame stabilization or the overall operation of the LSB.

Flame Oscillations

Flame crossing spectrum is a convenient means by which to investigate flame oscillations. The spectra shown in Figure 7 for open, enclosed, and enclosed constricted flames at $\bar{c} = 0.5$ are similar to those measured in other configurations (*e.g.*, *v*-flames and stagnating flames). The lack of discrete frequency peaks or spikes suggests that the enclosed LSB flame has no regular oscillation frequencies which could generate pressure disturbances. In contrast, the frequency spectra reported by Halthorne and Gouldin (1986) for enclosed premixed flames stabilized by co-swirl and by counter-swirl flames show both low (50 – 100 Hz) and high (400 – 500 Hz) frequency

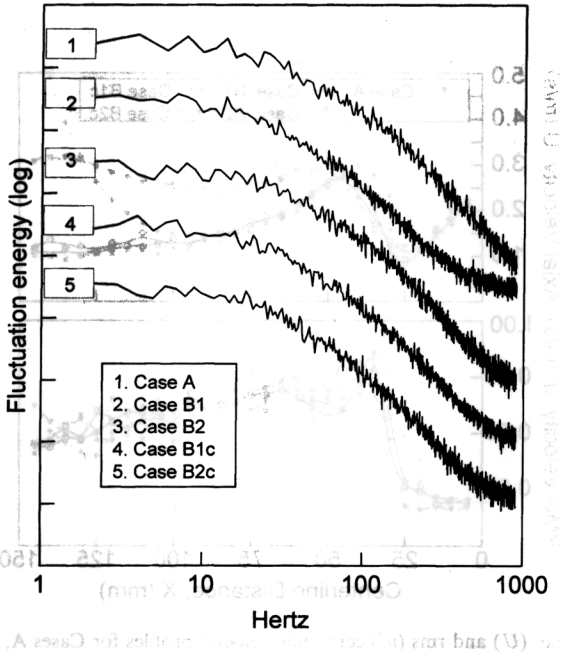

FIGURE 7 Flame crossing spectra from MSOD for $S_g = 0.05$, $U_\infty = 2.7$ m/s and $\phi = 0.80$.

oscillations. They attributed the high frequency oscillations to the instabilities of the reactant flow and the low frequencies to the movement of the recirculation zone. Without a recirculation zoe, the LSB does not generate the low frequencies that are often the source of the flame oscillations in enclosed premixed combustion systems.

A characteristic of the LSB that may explain its highly stable and quiet performance is the lack of large shear stresses in its flowfield. Using Eq. (3)

$$\frac{\overline{(U-\bar{U})*(V-\bar{V})}}{u_{\text{rms}} * v_{\text{rms}}} \tag{3}$$

the correlations for the three profiles in Figure 5 are −0.030, −0.055, and −0.009 for Cases A, B1, and B2 respectively. These velocity measurements show that the Reynolds stresses are essentially zero. This is not the case for flames stabilized in a TRZ where high shear stresses can lead to local quenching and thus variations in the heat release rate. Due to the absence of a TRZ or high shear stresses, the LSB flames are much less susceptible to disturbances caused by heat release variations, such as instability, noise, and vibration.

Evaluation for Water Heaters

The combustion chamber/heat exchanger in the water heater simulator was a 15 kW, mid-efficiency (rated at 82%), non-condensing unit which will produce a 10°C temperature rise with a flow rate of 15 liters/min. The LSB-fitted water simulator was tested from $\phi = 0.70$ to 0.90 at thermal inputs of 12, 15, and 18 kW with a water flow rate of 15 liters/min. In Figure 8(a), the thermal efficiency, ε, is shown to increase with ϕ. Between $0.70 \leq \phi \leq 0.80$, ε rises about 3% from 75% to 78%. For $\phi < 0.80$, the gain is less significant. Increasing the thermal input leads to a decrease in ε from a high of 81% at 12 kW ($\phi = 0.90$) to 78% at 18 kW. This decrease in ε was accompanied by an increase in flue gas temperature and is likely due to the non-optimal design of the rectangular heat exchanger *vis-a-vis* the round LSB. At 15 kW and $\phi = 0.80$, the LSB system had a $\varepsilon \approx 77\%$, which is comparable to the conventional system despite the lower flame temperatures generated by the lean premixture.

Figures 8(b) and (c) show CO and NO_x emissions which were sampled 500 mm above the heat exchanger. The CO and NO_x concentrations have

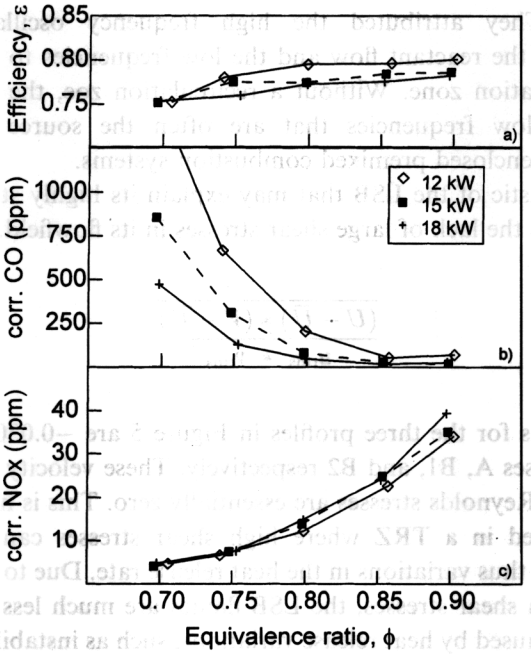

FIGURE 8 Efficiency (ε), CO, and NO_x emissions from the LSB water heater simulator for three thermal inputs. The original Telstar system had $\varepsilon = 82\%$, CO = 10 ppm and $NO_x = 90$ ppm.

been corrected to 3% O_2 according to Eq. (4) to account for different dilution levels.

$$X(\text{corrected to } 3\%\ O_2) = X(\text{measured}) * \frac{1 - 3.0/20.9}{1 - O_2\%/20.9} \tag{4}$$

In Figure 7(b), the CO concentrations at $\phi = 0.70$ show a dramatic decrease with increasing thermal inputs with CO = 1350 ppm at 12 kW while CO = 470 ppm at 18 kW. All three sets of data show CO emissions decreasing with increasing ϕ. Minimum levels were achieved between $0.85 \leq \phi \leq 0.90$, where CO = 60 ppm at 12 kW while CO $\approx$ 20–25 ppm at both 15 and 18 kW. Unlike the pulse combustor (Keller *et al.*, 1994) where CO levels are at least four times lower than those shown in Figure 7(b), the LSB has no flow recirculation to promote CO–CO_2 conversion. Moreover, the swirl air is a deterrent to this conversion as it dilutes the edges of the reactant flow and thus may lower the local ϕ below the flammability limit. This appears to be the cause of the exceedingly high levels of CO at the lower equivalence ratios.

The NO_x profiles shown in Figure 12(c) are typical of those measured in lean premixed laminar flames (Miller and Bowman, 1989) which decrease from 40–50 ppm near stoichiometry to below 5 ppm for $\phi < 0.7$. As the turbulent flames produced by the LSB are within the wrinkled flamelet regime, the local reaction rate of the flamelet, and hence the emission characteristics, are not expected to be influenced by turbulence. For all three thermal inputs of 12, 15 and 18 kW, NO_x emissions are lowest at $\phi = 0.70$ ($NO_x = 4$ ppm), increasing to 12–15 ppm at $\phi = 0.80$, and rising to $NO_x = 34–39$ ppm at $\phi = 0.90$. These emissions are slightly higher than those reported by Keller (1994) for a laboratory pulsed combustor operating at similar thermal inputs. The difference can again be explained by the exhaust gas recirculation process in the pulse combustor. Residual flue gas in the pulse combustor mixes with fresh premixture and serves as an inert diluent to lower flame temperature, thus reducing the production of NO_x through thermal generation. The data does not show a dependency of NO_x emissions with thermal input.

California has some of the most stringent air quality standards in the United States. Regulations stipulate that many water heaters, boilers, furnaces, and other combustion-related appliances are limited to NO_x emissions of less than 40 μg/kJ of useful output (Rule 1111, 1983; Rule 1121, 1995) as calculated using Eq. (5).

$$NO_x(\mu g/kJ) = \frac{3.6557e7 * NO_x(\text{ppm measured})}{(20.9 - O_2\%) * HHV * \varepsilon} \tag{5}$$

It is clear that the NO_x emissions from the LSB-retroffited system are substantially below the regulated limit of 40 μg/kJ. At $\phi = 0.8$, the LSB emits just 20% of the allowable limit. In comparison, NO_x emissions from the Telstar Spa Heater with the original partially premixed rack-burner are 65 μg/kJ. Although regulations limit CO emissions to 400 ppm for most natural gas applications, manufacturers prefer to limit CO emissions below 50 ppm due to human health concerns. Therefore, the optimum operating conditions for the LSB at 15 kW would be at $\phi = 0.85$ where the NO_x and

TABLE II Conversion of NO_x ppm to μg NO_x/kJ at 15 kW for the water heater simulator

ϕ	0.70	0.75	0.80	0.85	0.90
NO_x in ppm	2.6	5.2	9.4	19.3	28.2
O_2%	9.3	8.4	7.5	7.0	6.5
Efficiency, ε	0.750	0.775	0.775	0.785	0.785
μg of NO_x/kJ energy out	2.8	5.1	8.6	16.8	23.8

CO emissions equal 25 ppm (corrected to 3% O_2). With an $\varepsilon = 78.5\%$, the water heater simulator has a similar thermal efficiency compared to the commercial product but with substantially lower emissions.

During the course of these tests, other practical considerations such as gas supply pressure, fan-blower power requirement, swirl air supply pressure, ease of ignition, type of ignition sources, ignition source placement, and burner orientation have been investigated. Due to its open tube design, the LSB can be operated with a small 10 W electric blower, a natural gas supply pressure of only 0.75 kPa, and a swirl air supply pressure of < 1 kPa. Because the flame has no specific anchoring point, placement of the ignition source is not crucial. The reactants can be lit from above or from the side using a spark source or a glow plug. The flame propagates naturally to the stabilization position. This is unique in that many burners require the ignition source to be adjacent to the stabilizer. The LSB has been fired horizontally and up-side down with the flame remaining stable despite changes in the overall flame shape due to buoyancy effects. These orientation tests demonstrate the feasibility of using LSB in high efficiency systems where a condensing heat exchanger is placed underneath or off to the side of the burner.

This investigation has demonstrated that the lean premixed LSB can be a simple, economical and versatile burner technology for low emission, combustion systems. It is also clear that the emissions of CO preclude operating the LSB at ultra low NO_x conditions for $\phi < 0.8$. However, there are several methods that will further reduce the CO emissions from LSBs. One method is to use the combustion products or natural gas/air premixture for the swirl jets rather than compressed air. Another possibility is the use of a guide vane swirler to generate the divergent flow instead of the tangential swirl jets [Yegian, 1996 #26]. Other investigations are being pursued to investigate using LSBs in larger atmospheric combustion systems and pressurized, power generating systems.

CONCLUSION

Laboratory experiments have been performed to evaluate the feasibility of using a premixed, low-swirl burner (LSB) in atmospheric boilers and furnaces. To simulate the operating conditions and environment of these systems, the LSB was studied inside quartz cylinders of various diameters and lengths, as well as with and without an exhaust constriction. The effects of confinement and downstream flue constriction on the stabilization range,

flame stabilization mechanism, flowfield behavior, and flame osciallations were investigated by laser diagnostics.

The stabilization ranges as defined by the swirl numbers at blowoff and flashback were compared for different system configurations and thermal inputs. Increasing the exit tube length extends the stabilization range and increases the swirl requirement. There is no significant systematic change in either the flashback or blowoff limits due to flame enclosure. For higher thermal inputs, wider stabilization ranges are found. This implies that the LSB is amenable to scaling to even higher thermal inputs than were investigated in this paper.

The velocity data obtained by LDV measurements show that the divergent nature of the LSB adapts well to enclosures of different sizes. Enclosing the LSB had no observable effect on the basic flame stabilization mechanism. For flames enclosed in cylinders ($R_e/R = 3$) larger than the open flame, the overall flow features remained essentially unaffected. A smaller enclosure ($R_e/R = 2$) constrained the flow divergence and caused the mean strain rate upstream of the flame zone to decrease and the flame brush thickness to increase. Constricting the exhaust was found to affect only the flow downstream of the flame zone.

Flame crossing spectra for unenclosed and enclosed LSB flames were identical. The absence of spectral peaks indicates that the enclosed LSB has no discrete fluctuation frequencies. This suggests that the LSB may be less susceptible to instability, vibration and noise problems common to other enclosed premixed combustion systems.

Tests performed in a water heater simulator showed that the LSB has low NO_x emissions (5–40 ppm at 3% O_2) while maintaining comparable thermal efficiencies as current commercial units. These NO_x levels were independent of thermal input. However, CO concentrations were found to decrease with increasing thermal input and ϕ. At 15 kW, the optimum operating conditions was found to be at $\phi = 0.85$ with $NO_x = 25$ ppm, CO = 25 ppm and $\varepsilon = 79\%$. The emissions are well below current regulations. This study has demonstrated that the lean premixed LSB can be a simple, economical and versatile burner for low emission, atmospheric boilers and furnaces.

Acknowledgements

This work was performed under a Cooperative Research and Development Agreement with Teledyne Laars, Moorpark, California supported by the

Director, Office of Energy Research, Laboratory Technology Research of the U.S. Department of Energy under Contract No. DE-AC-03-76SF00098. Laboratory facility and diagnostics supported by the Director, Office of Energy Research, Chemical Sciences Division of the U.S. Department of Energy.

NOMENCLATURE

$\bar{c}$ = mean progress variable 0 in reactants, 1 in products

ϕ = equivalence ratio

δ = flame brush thickness

a = mean strain rate, dU/dx

ε = thermal efficiency of laboratory test station

$$\equiv \frac{\dot{m}_w * c_p * \Delta T_w}{\rho_f * \dot{m}_f * \text{HHV}} = \frac{\text{Energy transferred to water}}{\text{Chemical energy entering with fuel}}$$

$\dot{m}_w$ = mass flow rate of water

$\dot{m}_f$ = mass flow rate of fuel

ρ_f = density of natural gas = 0.6992 kg/m^3

c_p = specific heat of water = 4.18 kJ/kg/K

HHV = high heating value of natural gas = 38,400 kJ/m^3

ΔT_w = rise in water temperature

ℓ = length of exit tube

L_e = length of quartz enclosure

R = radius of exit tube = 26.4 mm

R_e = radius of quartz enclosure

R_f = radius of flue constriction

R_θ = radius of air injectors = 1.6 mm

S_g = swirl intensity $\equiv \frac{R_\theta * R * \pi}{A_\theta} \left(\frac{m_\theta}{m_t}\right)^2$

m_θ = tangential mass flow = cos (20^0) * mass of swirl air

m_t = total mass flow

A_θ = total area of injectors

S_l = laminar flame speed

U_∞ = reference flow velocity $\equiv (\dot{v}_a + \dot{v}_f)/(\pi R^2)$

$\dot{v}_a$ = volume of reactant air (liters/sec)

$\dot{v}_f$ = volume of fuel (liters/sec)

U, u' = mean and rms axial velocities (m/s)

V, v' = mean and rms radial velocities (m/s)

W, w' = mean and rms angular velocities (m/s)

References

Bedat, B. and Cheng, R. K. (1995) Experimental study of premixed flames in intense isotropic turbulence, *Combustion and Flame*, **100**(3), 485–494.

Bedat, B. and Cheng, R. K. (1996) Effects of buoyancy on premixed flame stabilization, *Combustion and Flame*, **107**(1–2), 13–26.

Beer, J. M. (1996) Low NO_x burners for boilers, furnaces and gas turbines; drive towards the lower bounds of NO_x emissions, *Combustion Science and Technology*, **121**(1–6), 169–191.

Beer, J. M. and Chigier, N. A. (1972) *Combustion Aerodynamics*, London, Applied Science Publishers Ltd.: 100–146.

Bowman, C. T. (1975) Kinetics of Pollutant Formation and Destruction in Combustion, *Progress in Energy Combustion Science*, **1**, 33–45.

Bowman, C. T. (1992) Control of combustion-generated nitrogen oxide emissions: Technology driven by regulation, *Twenty-fourth Symposium (International) on Combustion*, The Combustion Institute, pp. 1109–1117.

Chan, C. K. *et al.* (1992) Freely propagating open premixed turbulent flames stabilized by swirl, *Twenty-fourth Symposium (International) on Combustion*, The Combustion Institute, pp. 519–525.

Cheng, R. K. (1995) Velocity and scalar characteristics of premixed turbulent flames stabilized by weak swirl, *Combustion and Flame*, **101**(1–2), 1–14.

Cheng, R. K. *et al.* (1989) A comparison of the velocity and scalar spectra in premixed turbulent flames, *Combustion and Flame*, **78**(2), 205–222.

Chigier, N. A. and Chervinsky, A. (1966) Aerodynamic study of turbulent burning free jets with swirl, *Eleventh Symposium (International) on Combustion*, The Combustion Institute, pp. 489–499.

Claypole, T. C. and Syred, N. (1980) Effect of swirl burner aerodynamics on NO_x formation, *Eighteenth Symposium (International) on Combustion*, The Combustion Institute, pp. 81–89.

Halthore, R. N. and Gouldin, F. C. (1986) Laser scattering measurements for gas density in a swirling flow combustor, *AIAA Journal*, **24**(7), 1129–1136.

Heitor, M. V. *et al.* (1984) Influence of confinement on combustion instabilities of premixed flames stabilized an axisymmetric baffles, *Combustion and Flame*, **57**, 109–121.

Keller, J. O. *et al.* (1994) NO_x and CO emissions from a pulse combustor operating in a lean premixed mode, *Combustion and Flame*, **99**(3–4), 460–466.

Lilley, D. G. (1977) Swirl flows in combustion : a review, *AIAA Journal*, **15**(8), 1063–1078.

Miller, J. A. and Bowman, C. T. (1989) Mechanism and modeling of nitrogen chemistry in combustion, *Progress in Energy and Combustion Science*, **15**(4), 287–338.

O'Young, F. and Bilger, R. W. (1996) Measurement of scalar dissipation in premixed flames, *Combustion Science and Technology*, **113–114**, 393–411.

Richards, G. A. *et al.* (1997) A test device for premixed gas turbine oscillations, *Transactions of the ASME: Journal of Engineering for Gas Turbines and Power*, **119**, 776–782.

Rule, 1111 (1983) NO_x Emissions from Natural-Gas-Fired, Fan-Type Central Furnaces, South Coast Air Quality Mangement District.

Rule, 1121 (1995) Control of Nitrogen Oxides from Residential Type, Natural Gas-Fired Water Heaters, South Coast Air Quality Management District.

Schefer, R. W. *et al.* (1996) Effect of confinement on bluff-body burner recirculation zone characteristics and flame stability, *Combustion Science and Technology*, **120**(1–6), 185–211.

Sivasegaram, S. and Whitelaw, J. H. (1987) Oscillations in confined disk-stabilized flames. *Combustion and Flame*, **68**(2), 121–130.

Sivasegaram, S. and Whitelaw, J. H. (1991) The influence of swirl on oscillations in ducted premixed flames, *Combustion and Flame*, **85**(1–2), 195–205.

Syred, N. and Beers, J. M. (1974) Combustion in swirling flows: a review, *Combustion and Flame*, **23**, 143–201.

Williams, A. *et al.* (1992) The formation of NO_x in surface burners, *Combustion and Flame*, **89**(2), 157–166.

Yegian, D. T. and Cheng, R. K. (1996) Development of a vane-swirler for use in a low NO_x weak-swirl burner, *American Flame Research Committee International Symposium.*